ULTRASONIC SENSING SIMULATION OF CdTe SINGLE CRYSTAL GROWTH

Yichi Lu and Haydn N. G. Wadley
Intelligent Processing of Materials Laboratory
School of Engineering and Applied Science
University of Virginia
Charlottesville, Virginia 22903

INTRODUCTION

Today's infrared detector arrays consist of $Hg_{1-x}Cd_xTe$ deposited upon lattice matched $Cd_{1-x}Zn_xTe$ substrate wafers. Very high quality $Cd_{1-x}Zn_xTe$ crystals must be grown so that substrate wafer defects do not degrade the detector's performance. Usually, the $Cd_{1-x}Zn_xTe$ crystals are grown by a Bridgman technique in which a charge is melted in a cylindrical quartz ampoule and slowly withdrawn from the hot zone (at ~ 1100°C) of a furnace.[1] The best quality crystal is obtained from material solidified under plane front conditions.[2] This is difficult to achieve, and a need has arisen for insitu sensing of the growth process to characterize, and ultimately control, the interface shape.

One possible approach is ultrasonic velocity sensing. The ultrasonic time of flight (TOF) methods have been used successfully to measure the internal temperature field[3, 4] and the liquid-solid interface[5] during the solidification of metals and alloys. It is based on the relative transparency to ultrasound of many compound semiconductors (even at high temperatures), the strong dependence of ultrasonic velocity upon temperature and the discontinuous change in velocity upon melting (many systems exhibit velocity differences of 20 % or more between liquid and solid). With the emergence of laser ultrasonic transduction methods,[6] these concepts potentially can be applied in the harsh environment of a crystal grower without perturbing growth conditions.

The application of these concepts to $Cd_{1-x}Zn_xTe$ single crystal growth is complicated by the anisotropic nature of wave propagation. The TOF of an ultrasonic ray traversing the region of solidification in this case depends upon both the fraction of the path traversing solid material and its crystallographic orientation. The bending (refraction) of the ray path at the liquid-solid interface (which contributes to the path length and thus TOF) also depends on crystal orientation. We have sought to investigate the significance of these effects to various sensor designs. In particular, we have (1) computed the velocity surface for CdTe from its published room temperature elastic constants, (2) estimated the liquid velocity and set up representative models of the region of solidification, (3) calculated the path and TOF for rays traversing the region (using a 2-D ray tracing algorithm) and (4) used a nonlinear least squares algorithm to reconstruct the liquid-solid interface shape. Encouraging results have been found and several sensor designs appear feasible.

Review of Progress in Quantitative Nondestructive Evaluation, Vol. 12
Edited by D.O. Thompson and D.E. Chimenti, Plenum Press, New York, 1993

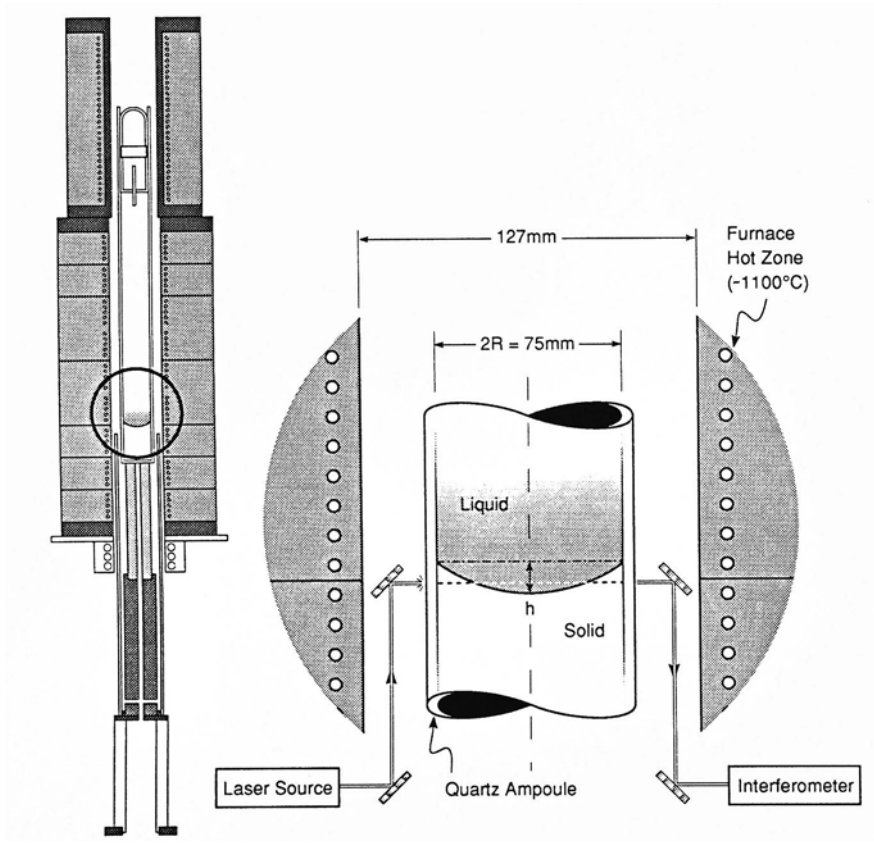

Fig. 1 A schematic arrangment of ultrasonic sensing in a vertical Bridgman furnace.

PROBLEM DEFINITION

A schematic diagram of a $Cd_{1-x}Zn_xTe$ crystal being grown by the Bridgman method is shown in Fig. 1. The solid-liquid interface, defined by its convexity ($\delta = h/2R$), can be ideally flat ($\delta = 0$), concave ($\delta = -0.5 \sim -0.1$) which is very deleterious for single crystal growth or convex ($\delta = 0.5 \sim 0.1$) which is often associated with high dislocation densities. The position of solidification within the furnace may also abruptly change for reasons that are not fully understood. Thus, the challenge posed is to find the optimal ultrasonic sensor that can determine interface convexity and measure the location of solidification within the furnace while not perturbing solidification. Experiments alone are a difficult, expensive and time consuming approach to this. We are using theoretical methods and numerical simulation to design and optimize the sensor approach.

Using modern interferometric transducers and laser generated ultrasound, the TOF can be readily obtained for rays that propagate between arbitrary source and receiver points on the ampoule boundaries. For an assumed geometry (ie ampoule diameter, crystal orientation, solid-liquid interface shape) and prescribed source and receiver points, we simulate ray propagation, determine the TOFs and then use this "data" to investigate the potential reconstruction accuracy for various sensor setups.

In general three mutually perpendicular wave modes (quasi-longitudinal, fast quasi-shear, and slow quasi-shear) can propagate in an anisotropic elastic body.[7] The group velocity for each mode differs from the phase velocity, and both depend upon the direction of propagation through the crystal lattice. We need to obtain the velocity surface for the plane traversed by the rays before we can determine the true ray paths and compute TOF values. The phase velocity is determined from the eigenvalues of the Christoffel equation :[7]

$$(\rho^{-1}c_{ijkl}n_k n_l - v^2\delta_{ij})d_i = 0 \qquad (1)$$

where ρ is the density, c_{ijkl} is the stiffness tensor, v is the phase velocity, d_i and n_i are components of the displacement and propagation vectors respectively, and δ_{ij} is Kronecker's delta. The components of the group velocity,v_{gi}, are given by[7]

$$v_{gi} = \frac{c_{ijkl}}{\rho} d_j d_l \frac{n_k}{v} \qquad (2)$$

The single crystal CdTe material has a cubic crystal structure. Figures 2a and 2b show the phase and the group velocity in the (111) plane of CdTe, where c_{11} = 53.51 GPa, c_{12} = 36.81 GPa, c_{44} = 19.94 GPa, the density for the solid phase ρ_s = 5.854 g/cm^3 (at 298 °K).[8] The velocity surfaces for the (001) section are similar to those already reported,[9] and are not reproduced here. The sound velocity in the liquid phase is taken to be 2.721 mm/μs, and the density ρ_l = 5.2 g/cm^3.

WAVE FRONT ANALYSIS

Wave fronts separate the ultrasonically disturbed region from the undisturbed one. The simplest wave front to be experimentally detected is the first arrival one. For anisotropic crystals, this corresponds to the quasilongitudinal wave since its velocity is the largest. We therefore study only the wave fronts of the quasi-longitudinal wave. Consider a cubic single crystal cylinder with a concentric cylindrical liquid core. The single crystal cylinder has an external radius R, and an inner liquid region of radius r. We consider the cases where the cylinder (z) axis, coincides in one case with the <001> and in another with the <111> direction.

Consider first the case in which the x, y, and z axes coincide with the [100], [010], and [001] directions, respectively, Fig. 3. An ultrasonic point source is located at (0, -R). For a ray propagating in the direction θ with respect to the [010] direction, we have

$$l = R\cos\theta - \sqrt{(R\cos\theta)^2 - (R^2 - r^2)} \qquad (3)$$

$$\phi_1 = \tan^{-1}\left(\frac{l\sin\theta}{R - l\cos\theta}\right) \qquad (4)$$

$$\psi_1 = \phi_1 + \theta \qquad (5)$$

where l is the distance between the source point and the point where the ray first touch the interface.

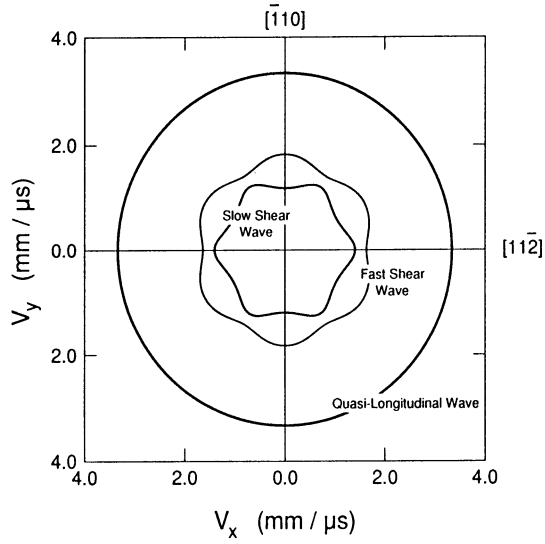

Fig. 2a The phase velocity in the (111) plane of CdTe.

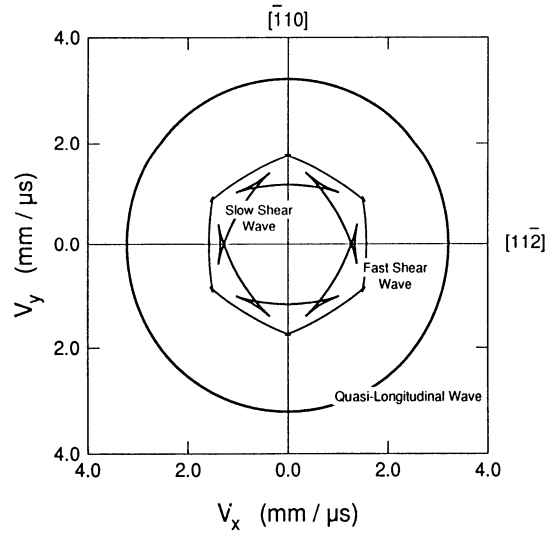

Fig. 2b The group velocity in the (111) plane of CdTe.

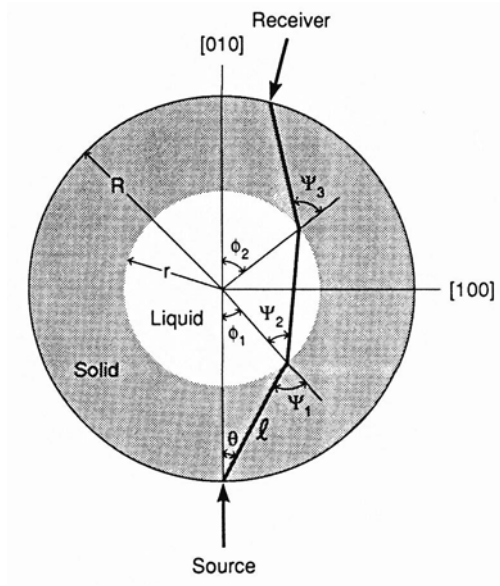

Fig. 3 An illustration for the ray path analysis.

The angle of refraction (ψ_2) at the solid-liquid interface is determined by Snell's law :

$$\frac{\sin\psi_2}{v_l} = \frac{\sin\psi_1}{v_{QL}(\theta)} \tag{6}$$

where v_l is the longitudinal wave velocity in the liquid phase, $v_{QL}(\theta)$ is the phase velocity of the ray propagating in the solid phase at an angle of θ with respect to the [010] direction. When the refracted ray exits the liquid at the liquid-solid interface we simultaneously invoke the Christoffel equation together with Snell's law to obtain the admissible angles of refraction and use the Poynting Vector to determine the correct refraction angle ψ_3.[10, 11]

We introduce a local coordinate system in which the x′ axis is tangential to the liquid-solid interface, and the y′ axis passes through the center of the liquid core. The angle ψ_2 is now the direction for the incident ray propagating in the liquid phase, and the angle ψ_3 gives the direction for the refracted ray propagating in the solid phase. The projection of the wavenumber k, where $k = \omega/v$, ω is the angular frequency, on the x′ axis must be the same on both sides of the interface:

$$k_{x'} = k_l \sin\psi_2 = k_{QL}(\psi_3) \sin\psi_3 \tag{7}$$

where $k_l = \omega/v_l$ is the wavenumber in liquid. When the z axis coincides with the [001] direction and the wave normal is perpendicular to that direction, the Christoffel equation can be written :

$$\begin{vmatrix} k^2\Gamma_{11} - \rho\omega^2 & k^2\Gamma_{12} \\ k^2\Gamma_{21} & k^2\Gamma_{22} - \rho\omega^2 \end{vmatrix} \begin{Bmatrix} d_1 \\ d_2 \end{Bmatrix} = 0 \tag{8}$$

where

$$k^2\Gamma_{11} = c_{11}(k_1 \sin\psi_2)^2 + c_{66}k^2_{y'} + 2c_{16}(k_1 \sin\psi_2)k_{y'} \quad (9a)$$

$$k^2\Gamma_{12} = c_{16}(k_1 \sin\psi_2)^2 + c_{26}k^2_{y'} + (c_{12} + c_{66})(k_1 \sin\psi_2)k_{y'} \quad (9b)$$

$$k^2\Gamma_{22} = c_{66}(k_1 \sin\psi_2)^2 + c_{22}k^2_{y'} + 2c_{26}(k_1 \sin\psi_2)k_{y'} \quad (9c)$$

d_1 and d_2 are components of the displacement vector ($d_3 = 0$). Substituting Eq. (9a-c) into Eq. (8) and solving the eigenvalue problem for Eq. (8) results in four solutions for $k_{y'}$: two for the refracted quasi-longitudinal wave, and two for the refracted quasi-shear wave. The eigenvector corresponding to each $k_{y'}$ is then obtained using Eq. (8). We choose the one for which the direction of the acoustic energy flow, determined by Eq. (2), is in the positive y' direction.

Figure 4 shows the calculated ray paths for a [001] crystal cylinder with an external radius R = 37.5 mm, and an inner liquid radius r = 7.5 mm. We see that there exists a critical incidence angle $\theta_c = \sin^{-1}(r/R)$. When $\theta > \theta_c$ no ray enters into the liquid core, and the ray paths are straight. Each ray that enters into the liquid core ($\theta < \theta_c$) is bent twice by the interface toward the center line ([010] direction). Those rays entering into the liquid core are bounded by two caustics. Between the caustic and the ray with the angle $\theta = \theta_c$ there is a shadow zone. Only diffracted rays can exist in the shadow zone. We notice that locating the boundaries of the shadow zone may be one way to determine the interface radius.

Figure 5 shows the quasilongitudinal wave fronts obtained by connecting points on the ray paths with the same TOFs. After passing through the liquid core, the edges of the wave fronts are folded by the interface. The edges are folded forward since for the (001) plane, the ultrasound velocity is larger in the [110] direction, and the rays corresponding to the edges of the wave fronts are propagating more closely in this direction. Similar results can be obtained for [111] crystal cylinders.

RECONSTRUCTION RESULTS

Every and Sachse have shown[12] that when only quasi-longitudinal TOF data is available, only a partial set of the elastic constants of anisotropic materials can be recovered no matter which ray paths are used. For cubic materials, this set includes c_{11} and $(c_{12}+2c_{44})$. In the crystal growth situation, the elastic constants would fortunately be known. We need only to recover the interface radius, ultrasound velocity in the liquid phase (which gives its temperature), and the crystal orientation. One approach is the nonlinear least squares method.[13] Since both the phase and group velocities for the quasi-longitudinal wave in the (111) plane are isotropic, the crystal orientation for this plane will not be recovered if only the quasi-longitudinal TOF data is used. Table I shown below lists results for such a reconstruction for the (001) and (111) planes of a crystal containing liquid with inner radius r = 20 mm. Simulated "measured" TOF data was used for the reconstruction by adding ± 50 nsec "noise" to the calculated TOF data from the group velocity. A total of 21 TOF data were used with $-45.0^\circ \le \theta \le 45.0^\circ$. For the (001) plane, the crystal orientation was defined as the angle between the [010] direction and the y coordinate of the laboratory reference frame.

The reconstructions have remarkably well recovered the unknowns in the models. They suggest that a set of TOF values collected on a cross sectional slice through the region of solidification may indeed provide a way to infer liquid-solid interface geometry. Repeating the measurements at other axial locations (with different values of r) may then allow a 3-D mapping of the interface. The calculation's principal limitations are the use of 2-D ray tracing algorithm and the absence of reliable ultrasonic velocities for the high temperature solid and the liquid. Future work will address these issues.

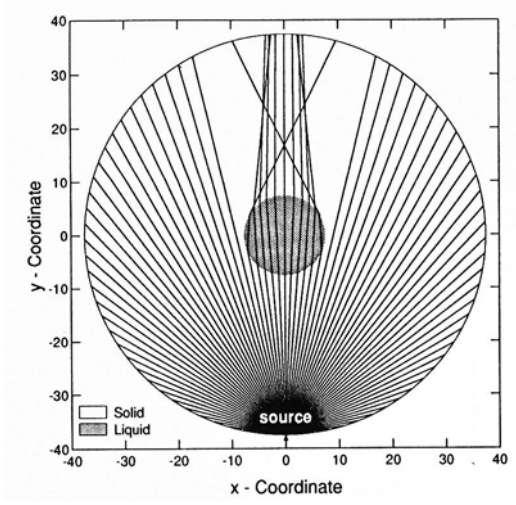

Fig. 4 The calculated ray paths for a [001] crystal cylinder, R = 37.5 mm, r = 7.5 mm.

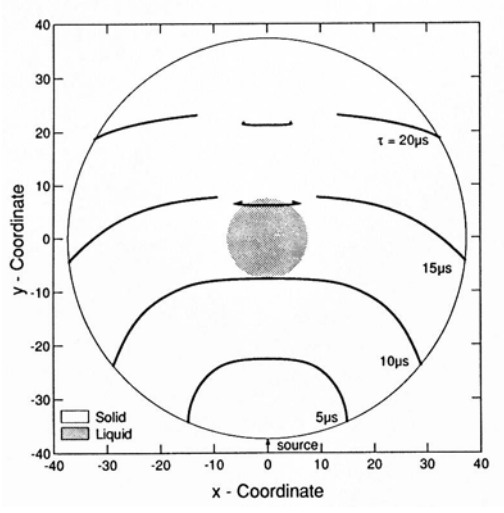

Fig. 5 The quasilongitudinal wave fronts for a [001] crystal cylinder, R = 37.5 mm, r = 7.5 mm.

Table I Reconstructed model parameters using a nonlinear least squares method, with ±50 nsec noise

	Interface Radius	Liquid Velocity	Orientation
Exact model values	r = 20.0 mm	2.7210 mm/μs	30°
Reconstructed values, (001) plane	r = 19.9489 mm	2.7261 mm/μs	28.35°
Reconstructed values, (111) plane	r = 21.8009 mm	2.7444 mm/μs	—

ACKNOWLEDGEMENTS

This work has been conducted as part of the research of the Infrared Materials Producibility Program that includes Johnson Matthey Electronics, Texas Instruments, II-VI Inc., Loral, BDM Int. and the University of Virginia. We are grateful for many helpful discussions with our collegues in these organizations. The work has been supported by DARPA/CMO under contract MD A972-91-C-0046 monitored by Raymond Balcerak.

REFERENCES

1. M. Pfeiffer and M. Muhlberg, J. Cryst. Growth, 118, 269, (1992).
2. T. Fu and W. R. Wilcox, J. Cryst. Growth, 48, 416, (1985).
3. H. N. G. Wadley, S. J. Norton, F. A. Mauer and B. D. Droney, Proc. Roy. Soc. Phil. Trans. A32C, 341, 1986.
4. H. N. G. Wadley, S. J. Norton, F. A. Mauer and B. D. Droney, Proc. Alum. Assoc. Workshop on Sensors, (Aluminum Assoc., Washinton, DC, 1986, p73.)
5. F. A. Mauer, S. J. Norton, Y. Grinberg, D. Pitchure and H. N. G. Wadley, Met. Trans. A22B, 467, 1991.
6. Yichi Lu, Jeffrey A. Goldman and Haydn N. G. Wadley, *Review of Progress in Quantitative Nondestructive Evaluation*,eds., D. O. Thompson and D. E. Chimenti, Plenum Press, New York, 11(A), 789, (1992).
7. F. I. Fedorov, *Theory of Elastic Waves in Crystals*, (Plenum Press, New York, 1968).
8. D. H. Chung and W. R. Buessem, J. Appl. Phys., 38, 2535, (1967).
9. B. A. Auld, *Acoustic Fields and Waves in Solids*, (John Wiley & Sons, New York, 1973), Vol. 1, Chap. 3D.
10. A. Atalar, J. Acoust. Soc. Am. 73, 435, (1983).
11. O. Ankan, E. Telatar and A. Atalar, J. Acoust. Soc. Am. 85, 1, (1989).
12. W. Press, B. Flannery, S. Teukolsky, and W. Vetterling, *Numerical Recipes*, (Cambridge University Press, New York, 1989).
13. A. G. Every and W. Sachse, Ultrasonics, 30(1), 43-48, (1992).